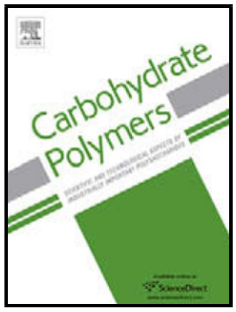

Title: An improved approach for evaluating the semicrystalline lamellae of starch granules by synchrotron SAXS

Author: Binjia Zhang Fengwei Xie David K. Wang Siming Zhao Meng Niu Dongling Qiao Shanbai Xiong Fatang Jiang Jie Zhu Long Yu

PII: S0144-8617(16)31370-4
DOI: http://dx.doi.org/doi:10.1016/j.carbpol.2016.12.002
Reference: CARP 11808

To appear in:

Received date: 29-8-2016
Revised date: 24-11-2016
Accepted date: 1-12-2016

Please cite this article as: Zhang, Binjia., Xie, Fengwei., Wang, David K., Zhao, Siming., Niu, Meng., Qiao, Dongling., Xiong, Shanbai., Jiang, Fatang., Zhu, Jie., & Yu, Long., An improved approach for evaluating the semicrystalline lamellae of starch granules by synchrotron SAXS.*Carbohydrate Polymers* http://dx.doi.org/10.1016/j.carbpol.2016.12.002

An improved approach for evaluating the semicrystalline lamellae of starch granules by synchrotron SAXS

Binjia Zhang[a,e], Fengwei Xie[c], David K. Wang[c], Siming Zhao[a], Meng Niu[a], Dongling Qiao[b,*], Shanbai Xiong[a], Fatang Jiang[b], Jie Zhu[d], Long Yu[e]

[a] *Key Laboratory of Environment Correlative Dietology (Ministry of Education), College of Food Science and Technology, Huazhong Agricultural University, Wuhan 430070, China*

[b] *Glyn O. Philips Hydrocolloid Research Centre at HUT, Hubei University of Technology, Wuhan 430068, China*

[c] *School of Chemical Engineering, The University of Queensland, Brisbane, Qld 4072, Australia*

[d] *College of Chemistry and Environmental Engineering, Dongguan University of Technology, Dongguan 523808, China*

[e] *Guangdong Province Key Laboratory for Green Processing of Natural Products and Product Safety, South China University of Technology, Guangzhou 510640, China*

[*] Corresponding author. *E-mail address*: qdttkl@163.com (D. Qiao)

Highlights:

- ✓ An improved method was developed for analyzing starch semicrystalline lamellae
- ✓ The proportion of the lamellae within the starch granule was calculated
- ✓ The profile of linear correlation function was largely improved
- ✓ The lamellar parameters of starch were obtained with increased accuracy

Nomenclature

WMS, waxy maize starch

RMS, regular maize starch

GMS, Gelose 50 high-amylose maize starch

PS, potato starch

SAXS, small-angle X-ray scattering

WAXS, wide-angle X-ray scattering

φ_c, the volume fraction of crystalline lamellae within semicrystalline lamellae

d, the thickness of semicrystalline lamellae for starch

d_c, the thickness of crystalline lamellae for starch

d_a, the thickness of amorphous lamellae for starch

$\Delta\rho$, the electron density difference between the crystalline and amorphous lamellae of starch

P_{SL}, the proportion of the semicrystalline lamellae within the starch granule

PL+B, power-law scattering (*PL*) plus scattering background (*B*)

X_c, the relative crystallinity of starch

$L(r)$, linear correlation function

α, power-law exponent

A_{peak}, area under the net lamellar peak of the SAXS pattern for starch

A_{total}, total scattering area of the SAXS pattern for starch

A_{PL+B}, area under the *PL+B* profile of the SAXS pattern for starch

$R_{X/\varphi}$, the ratio of X_c to φ_c

Abstract: A fitting method combined with a linear correlation function was developed as an improved approach for the SAXS analysis of the semicrystalline lamellae of starch granules. Using a power-law function with two Gaussian plus Lorentz functions, the SAXS pattern was resolved into sub-patterns of the net lamellar peak and the power-law scattering plus scattering background (*PL+B*). The ratio of the net lamellar peak area (A_{peak}) to the total scattering area (A_{total}) was proposed equal to the proportion of the lamellae within the starch granule (P_{SL}). Along with this fitting method, we obtained a better profile of linear correlation function, with the elimination of the interference of non-lamellar amorphous starch (*i.e.*, amorphous growth rings). Then, we could accurately calculate the lamellar parameters, *e.g.*, P_{SL}, the thicknesses of semicrystalline (d), crystalline (d_c) and amorphous (d_a) lamellae, and the volume fraction (φ_c) of crystalline lamellae within semicrystalline lamellae. Quantitative analysis revealed that P_{SL} was positively correlated with the crystallinity (X_c) of starch. It was confirmed that the distribution of lamellar thickness was more important than the starch botanical origin in affecting the validity of the developed fitting method. We also proposed a criterion to test the validity of the proposed method. Specifically, the total SAXS pattern should be mostly tangent to the profile of *PL+B* at a high q tail (close to 0.2 $Å^{-1}$).

Keywords: *starch; granule; semicrystalline lamellae; X-ray scattering; methodology*

Chemical compounds studied in this article

Starch (PubChem CID: 24836924); Water (PubChem CID: 962)

1. Introduction

As the main storage carbohydrate in higher plants, starch is normally used as a food ingredient providing energy for humans (Juansang, Puttanlek, Rungsardthong, Puncha-arnon & Uttapap, 2012). Also, starch has attracted huge interest in the development of functional foods (Fuentes-Zaragoza et al., 2011), bioactive carriers (Pu, Chen, Li, Xie, Yu & Li, 2011) and biomaterials (Situ, Li, Liu & Chen, 2015). There are two kinds of starch polymers, *i.e.*, amylose and amylopectin (Jiang, Gao, Li & Zhang, 2011; Liu, Halley & Gilbert, 2010). These two biopolymers are organized on multiple scales in the starch granule to form its semicrystalline structure, including the whole granule, the growth rings, the semicrystalline lamellae and the crystallites (Buleon, Colonna, Planchot & Ball, 1998; Luengwilai & Beckles, 2009; Perez & Bertoft, 2010; Pikus, 2005; Zhang et al., 2015). The semicrystalline structural features of starch such as crystallinity and lamellar ordering are crucial in the determination of the physicochemical properties, *e.g.*, digestibility (Blazek & Gilbert, 2010; Lopez-Rubio, Flanagan, Shrestha, Gidley & Gilbert, 2008) and thermal behaviors (Liu, Xie, Yu, Chen & Li, 2009; Xie, Halley & Avérous, 2012). Thus, to understand a specific functionality of starch, analytical techniques should be used to accurately evaluate the semicrystalline structure of starch.

Small-angle X-ray scattering (SAXS) is a powerful technique for the characterization of starch lamellae on the nanoscale (Doutch & Gilbert, 2013; Lopez-Rubio, Flanagan, Gilbert & Gidley, 2008; Zhang, Chen, Li, Li & Zhang, 2015). Particularly, the average thickness (d) of the semicrystalline lamellae is normally calculated with Woolf-Bragg's equation (Zhang, Chen, Li, Li & Zhang, 2015; Zhang et al., 2014). Additional lamellar parameters can be obtained using the paracrystalline model (Cameron & Donald, 1993a, b), the liquid-crystalline model (Daniels & Donald, 2004) and the linear correlation function (Zhang, Chen, Li, Li & Zhang, 2015; Zhang et al., 2015). Those parameters include the thicknesses of crystalline (d_c) and amorphous (d_a) lamellae, the electron density difference ($\Delta\rho$) between the crystalline and amorphous lamellae, and the volume fraction (φ_c) of the

crystalline lamellae within the semicrystalline lamellae. The distribution of lamellar thickness has also been studied using the interface distribution function (Cardoso & Westfahl, 2010).

However, though numerous studies have evaluated the lamellar structure of starch, the relative proportion (named as P_{SL}) of the semicrystalline lamellae within the starch granule has never been calculated. Also, among above mentioned methods, the linear correlation function is fairly straightforward, as no predefined assumptions of the starch structure are needed. Nonetheless, the non-lamellar amorphous starch (*i.e.*, amorphous growth rings) exists as a third-phase fraction in the starch granule. The third-phase starch reduces the accuracy of the linear correlation function to calculate the parameters of the two-phase semicrystalline lamellae. This interference prevents us from establishing accurate links between the functionalities and the semicrystalline features of starch, which is undesired for the rational design of starch products with tailored performance. Thus, if the scattering arising from the semicrystalline lamellae could be properly resolved from the total SAXS pattern of starch, it would be possible to calculate P_{SL}. Also, using the net scattering of the lamellae, the lamellar parameters of starch would be accurately obtained from the linear correlation function, due to the elimination of the interference of the third-phase starch.

To this end, a fitting equation based on a power-law function with two Gaussian plus Lorentz functions was developed to aid the decomposition of starch SAXS pattern into sub-patterns of the net lamellar peak and a profile of power-law scattering plus scattering background (*PL+B*). Then, the profile of linear correlation function was largely improved using the fitted net scattering for starch lamellae. Based on this, we obtained not only P_{SL} but also other lamellar parameters (*e.g.*, d, d_c, d_a and φ_c) with increased accuracy.

2. Materials and methods

2.1 Materials

Waxy maize starch (WMS), regular maize starch (RMS) and Gelose 50 high-amylose maize starch (GMS) were purchased from Penford Australia Ltd. (Lane Cove, NSW Australia). WMS, RMS and GMS had amylose contents of *ca*. 3%, 24% and 56%, respectively, as measured using an iodine colorimetric method (Tan, Flanagan, Halley, Whittaker & Gidley, 2007). Potato starch (PS) (amylose content, *ca*. 36%) was supplied by Avebe (Netherlands). The moisture content of starch was determined using a moisture analyzer (MA35, Sartorius Stedim Biotech GmbH, Germany).

2.2 Small/Wide Angle X-ray Scattering (SAXS/WAXS)

SAXS/WAXS measurements with 1s acquisition were performed on the SAXS/WAXS beam-line (flux, 10^{13} photons/s) installed at the Australian Synchrotron (Clayton, Australia) at a wavelength $\lambda = 1.54$ Å. A slight overlap in q was established, and the configuration covered $0.015 < q < 2.9$ Å^{-1} simultaneously. The scattering vector, q, was defined as $q = 4\pi\sin\theta/\lambda$, where 2θ is the scattering angle and λ is the wavelength of the X-ray source. The 2D scattering patterns were collected using a Pilatus 1M camera (active area 169 × 179 mm and pixel size 172× 172 μm) and a Pilatus 200K camera (active area 169× 33 mm and pixel size 172 × 172 μm). The Scatterbrain software was used to acquire the 1D data from the 2D scattering patterns. The starch slurries with a starch concentration of 40wt% were used as the samples, which were prepared by adding a desired amount of water to the starch. The scattering of pure water with a Kapton tape (5413 AMBER 3/4IN X 36YD, 3M, USA) on the stage window was used as the background data. All data were background subtracted and normalized using the Scatterbrain software. In particular, the background subtraction was conducted with care through a subtraction between the scattering of the starch slurry with Kapton tape and the scattering of pure water with Kapton tape. Each test was carried out in triplicate to acquire reliable SAXS/WAXS data.

The data in the range of $0.28 < q < 2.8$ Å^{-1} (*ca.* $4° < 2\theta$ for Cu Kα < 40°) were used as the WAXS patterns. The relative crystallinity (X_c, %) of starch was calculated using the PeakFit software (Ver. 4.12), according to Eq. (1).

$$X_c = \frac{\sum_{i=1}^{n} A_{ci}}{A_t} \quad (1)$$

In which, A_{ci} is the area under each crystalline peak with index i, and A_t is the total area of the WAXS pattern.

The data in the range of $0.015 < q < 0.20$ Å^{-1} were used as the SAXS patterns. The linear correlation function $L(r)$, as given in Eq. (2) (below) and **Fig. S1** (see the supplementary data), was used to calculate the parameters of semicrystalline lamellae, with Eq. (3).

$$L(r) = \frac{\int_0^\infty I(q)q^2\cos(qr)\mathrm{d}q}{\int_0^\infty I(q)q^2\mathrm{d}q} \quad (2)$$

$$T = d\varphi_c(1 - \varphi_c) \quad (3)$$

Here, r (nm) is the distance in real space. T is the insection of the linear region on $L(r)$ with the abscissa ($L(r) = 0$) (*cf.* **Fig. S1** in supplimentary data); d is the second maximum of $L(r)$ (*i.e.*, the average thickness of the semicrystalline lamellae); φ_c is the volume fraction of the crystalline lamellae within the semicrystalline lamellae. **Fig. S1** also shows a parameter d_a, representing the average thickness of amorphous lamellae, which is acquired by the solution of the linear region and the flat $L(r)$ minimum. Then, d_c, the average thickness of crystalline lamellae is obtained by $d_c = d - d_a$.

2.3 Statistical analysis

Data were expressed as means ± standard deviations (SD), and were analyzed by the one-way ANOVA and multiple comparison tests with a least significant difference using IBM SPSS software version 20.0 (Chicago, IL, USA). A statistical difference of $P < 0.05$ was considered to be significant.

3. Results and discussion

3.1 Synchrotron WAXS analysis

Fig. 1A shows the WAXS patterns of the starches, *i.e.*, WMS, RMS, GMS, and PS. Expectably, while WMS and RMS showed a typical A-type crystalline structure with intense peaks at *ca.* 1.07 and 1.63 $Å^{-1}$, and an unresolved doublet at *ca.* 1.21 and 1.28 $Å^{-1}$; GMS and PS displayed a B-type crystalline structure with the strongest peak at around 1.21 $Å^{-1}$, a characteristic peak at *ca.* 0.40 $Å^{-1}$, and several smaller peaks at *ca.* 1.07, 1.42, 1.56 and 1.70 $Å^{-1}$. The results of the relative crystallinity (X_c) are included in **Table 1**, in which the value of X_c ranged from *ca*. 22% to 45%. This WAXS analysis was aimed at aiding the development of a new method below, rather than providing new insights into the crystalline nature of starch.

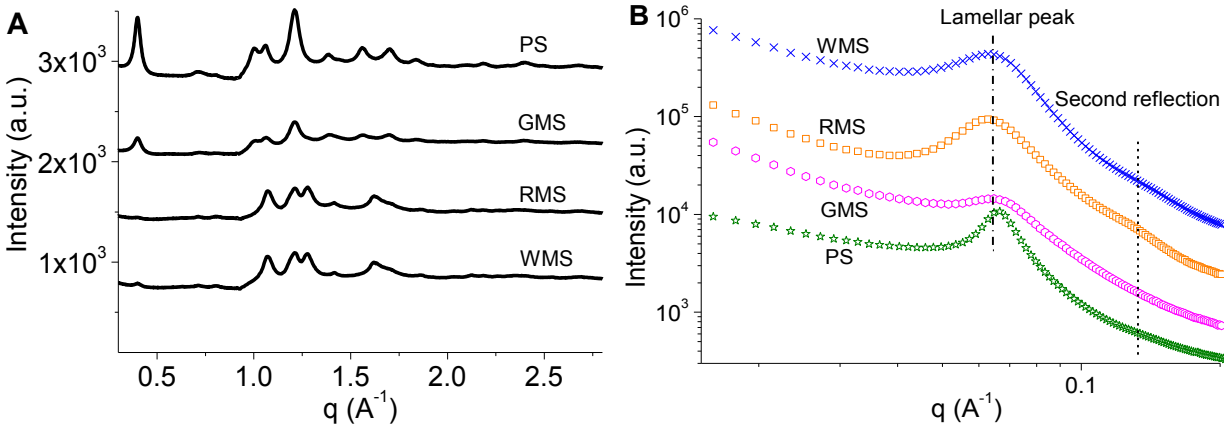

Fig. 1 WAXS ($0.028 < q < 2.8$ $Å^{-1}$, or *ca*. $4° < 2\theta$ for Cu Kα < 40°) (A) and SAXS (B) patterns for waxy maize starch (WMS), regular maize starch (RMS), Gelose 50 high-amylose maize starch (GMS), and potato starch (PS).

Table 1 Crystalline and lamellar parameters of starch granules. [A]

		WMS	RMS	GMS	WMS (b)	PS
	X_c (%)	45.44±0.85[a]	44.39±0.78[a]	22.22±1.15[c]	45.44±0.85[a]	39.36±1.13[b]
Fitting [B]	α	1.68±0.06[e]	1.98±0.03[b]	1.77±0.02[d]	2.36±0.00[a]	1.85±0.00[c]
	A_{total} (a.u)	713.30±29.12[a]	335.17±17.33[c]	221.28±10.65[d]	713.30±29.12[a]	491.39±19.89[b]
	A_{PL+B} (a.u)	397.52±13.75[a]	135.42±6.56[e]	155.03±7.30[d]	274.60±10.06[b]	219.37±9.07[c]
	A_{peak} (a.u)	315.78±15.37[b]	199.76±11.77[d]	66.25±3.35[e]	441.80±19.06[a]	273.78±10.82[c]
	P_{SL} (%)	44.26±0.35[d]	59.58±0.43[b]	29.94±0.07[e]	61.93±0.14[a]	55.71±0.05[c]
1D [C]	d (nm)	-	9.15±0.00[c]	9.18±0.00[b]	9.28±0.00[a]	9.08±0.02[d]
	d_a (nm)	-	2.48±0.01[c]	2.63±0.00[b]	2.62±0.01[b]	2.78±0.01[a]
	d_c (nm)	-	6.67±0.01[a]	6.55±0.00[b]	6.66±0.01[a]	6.30±0.01[c]
	φ_c (%)	-	73.12±0.26[a]	71.72±0.19[b]	71.28±0.31[b]	68.69±0.13[c]
	$R_{X/\varphi}$ (%)	-	60.71±0.85[b]	30.98±1.52[d]	63.56±1.19[a]	57.30±1.53[c]

[A] WMS, waxy maize starch; RMS, regular maize starch; GMS, Gelose 50 high-amylose maize starch; PS, potato starch; WMS (b), waxy maize starch with secondary fitting. Parameter obtained by WAXS: X_c, relative crystallinity.

[B] Parameters obtained using the proposed fitting method based on Eq. (4), *i.e.*, a power-law function with two Gaussian plus Lorentz functions: α, power-law exponent; A_{total}, total area under the whole SAXS pattern; A_{PL+B}, area under the profile of power-law (PL) scattering plus scattering background (B); A_{peak}, area under the net lamellar peak profile; P_{SL}, proportion of the semicrystalline lamellae within the starch granule, which is proposed equal to the ratio of A_{peak} to A_{total}.

[C] Parameters obtained by linear correlation function transformed from the fitted data of the net lamellar peak: d, the thickness of semicrystalline lamellae; d_a, the thickness of amorphous lamellae; d_c, the thickness of crystalline lamellae; φ_c, the volume fraction of crystalline lamellae within semicrystalline lamellae; $R_{X/\varphi}$, the ratio of X_c to φ_c.

3.2 Establishment of a new method for evaluating starch semicrystalline lamellae

3.2.1 Decomposition of the synchrotron SAXS pattern

Fig. 1B shows the SAXS patterns of WMS, RMS, GMS and PS. The starches showed a well-defined SAXS peak at *ca*. 0.065 $Å^{-1}$, corresponding to the semicrystalline lamellae (Cai & Shi, 2013; Zhang et al., 2014). Also, an additional less-resolved peak at *ca*. 0.13 $Å^{-1}$ was seen for WMS and RMS, which was ascribed to a second order reflection from the semicrystalline lamellae. This modest reflection has also been found for other starches such as tapioca starch (Blazek & Gilbert, 2010). Nonetheless, this reflection did not emerge for GMS and PS, presumably due to the fact that the scattering of the lamellar structure masked its second order reflection that was relatively weak.

Hence, two Gaussian plus Lorentz functions (with a power-law function), as shown in Eq. (4), were used to fit the lamellar peak and its second order reflection.

$$I(q) = B + Pq^{-\alpha} + f_1 * G_1(q) + (1 - f_1) * L_1(q) + f_2 * G_2(q) + (1 - f_2) * L_2(q) \quad (4)$$

In this equation, the first term B is the scattering background; the second term is the power-law function where P is the power-law prefactor and α is the power-law component; the third/fifth and fourth/sixth terms are the Gaussian ($G_1(q)$ or $G_2(q)$) and Lorentz ($L_1(q)$ or $L_2(q)$) functions, respectively, which describing the lamellar peak at around 0.65 $Å^{-1}$ or the second order reflection peak; f_1 and f_2 are the prefactors for the two peaks, respectively. Besides, the Gaussian $G_x(q)$ and Lorentz $L_x(q)$ functions are detailed in Eq. (5) and (6), respectively.

$$G_x(q) = \frac{A_x\sqrt{\ln 4}}{W_x\sqrt{\pi/2}} \exp\left(-\frac{2\ln 4(q - q_x)^2}{{W_x}^2}\right) \quad (5)$$

$$L_x(q) = \frac{2A_x}{\pi} * \frac{2W_x}{4(q - q_x)^2 + {W_x}^2} \quad (6)$$

Here, A_x is the peak area, W_x (Å^{-1}) the peak width at half-maximum in reciprocal space, and q_x (Å^{-1}) the peak center position; and x = 1 and x = 2 correspond to the lamellar peak and the second order reflection, respectively. Data fitting was performed using the least-squares refinement in the Origin8 software (OriginLab. Inc., USA).

In the following, the starches from the same botanical origin, *i.e.*, WMS, RMS and GMS, were selected for the method establishment. PS was mainly used in the section 3.5 to verify the validity of the established method for analyzing starches from different botanic origin origins. The fit curves for the SAXS data of WMS, RMS and GMS are shown in **Fig. 2**. The reduced *chi* square was 133.3 (WMS), 16.0 (RMS), and 29.9 (GMS), respectively, with an adjusted R^2 higher than 0.999. This indicates that the SAXS patterns of these maize starches were well fitted using the proposed Eq. (4).

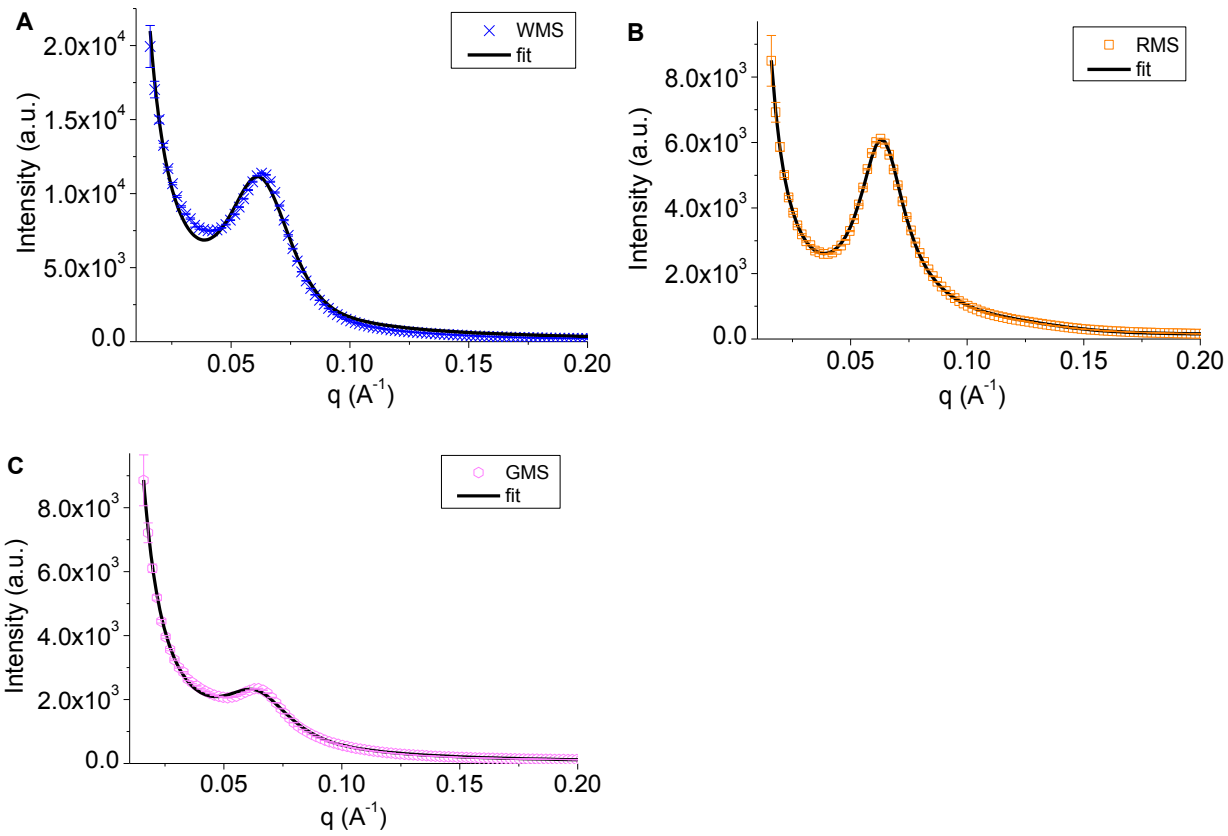

Fig. 2 SAXS patterns and their fit curves for waxy maize starch (WMS), regular maize starch (RMS), and Gelose 50 high-amylose maize starch (GMS).

As reported previously (Blazek & Gilbert, 2010; Cameron & Donald, 1993a, b), the starch granule can be seen as a finite stack of semicrystalline lamellae embedded in a medium of non-lamellar amorphous background (*i.e.*, amorphous growth rings); the lamellar peak closely relates to the semicrystalline lamellae, and thus the isolated change in amorphous background induces no variations in the peak intensity. Here, along with the fitting based on Eq. (4), we separated the whole SAXS pattern for starch into the sub-patterns of a net lamellar peak and the power-law scattering plus scattering background (*PL+B*). The net lamellar peak, in fact, corresponded to the fitted scattering of Gaussian plus Lorentz functions in Eq. (4). The rest *PL+B*, *i.e.*, power-law scattering ($Pq^{-\alpha}$) plus scattering background (*B*) in Eq. (4), should be mainly related to the non-lamellar amorphous background. Thus, we propose that the proportion (P_{SL}) of the semicrystalline lamellae within the starch granule equates to the ratio of the net lamellar peak area (A_{peak}) to the total area (A_{total}) of the SAXS pattern.

The profile of net lamellar peak and the *PL+B* profile resolved from the original SAXS patterns of the starches are collected in **Fig. S2** (see supplementary data). A_{total}, A_{peak} and A_{PL+B} (the area under the *PL+B* profile) were integrated from the corresponding profiles in **Fig. S2** using the Origin 8 software and the results are recorded in **Table 1**. It is seen that P_{SL}, *i.e.*, the ratio of A_{peak} to A_{total}, was larger than X_c for RMS and GMS but smaller than X_c for WMS. Actually, the crystallites in the untreated granule starch are mainly aligned in the crystalline lamellae to construct the semicrystalline lamellae with the lamellar amorphous starch. The value of P_{SL} should be higher than that of X_c. Thus, the result of P_{SL} for WMS was not reasonable. This contradiction needs a further clarification.

Fig. S3 (see the supplementary data) shows the comparison between the SAXS patterns and their *PL+B* profiles. For RMS and GMS, the *PL+B* profile almost touched the SAXS pattern at a high *q* tail (close to 0.2 $Å^{-1}$) without intersection, whereas for WMS, this profile intersected the SAXS pattern. That is, the above fitting for WMS allocated part of the scattering from the lamellar structure

into the profile of *PL+B*, leading to a smaller P_{SL} than its real value. Therefore, when the fitted profile of *PL+B* was approximately tangent to the total SAXS pattern at the high *q* tail, the scattering of the lamellar structure could be reasonably resolved from the original SAXS pattern using the proposed method. With this rule as a criterion, the SAXS pattern of WMS (recorded as WMS (b)) was again fitted using Eq. (4) (see **Fig. 3**). Then, like for the results of RMS and GMS, the P_{SL} of WMS (b) was greater than its X_c (**Table 1**).

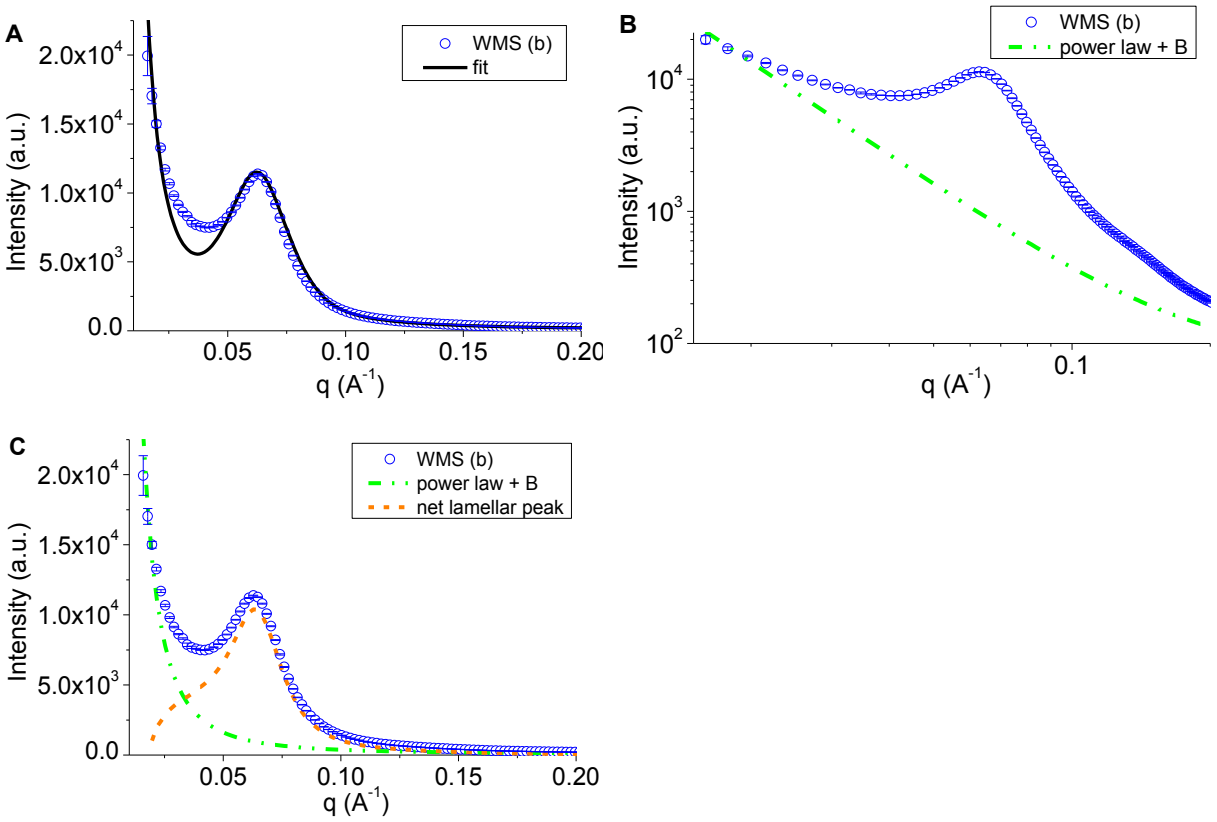

Fig. 3 SAXS pattern and its fit curve (A), SAXS pattern and its profile of power-law scattering *PL* plus scattering background *B* (B), decomposition of the SAXS pattern into sub-patterns of the net lamellar peak and *PL+B* (C), for waxy maize starch with secondary fitting (WMS (b)).

3.2.2 *Improvement of the profile of linear correlation function*

As discussed in the introduction, the linear correlation function is fairly straightforward for the characterization of starch lamellar paramters. However, the non-lamellar amorphous starch exists as a third-phase fraction in the starch granule, which evidently increases fluctuations of the linear correlation function profile and thus reduces the accuracy of the resultant parameters of the two-phase semicrystalline lamellae of starch. Thus, we further attempted to improve the profile of linear correlation function using the fitted net lamellar peak from the whole SAXS pattern without *PL+B* associated with non-lamellar starch.

Fig. 4 shows the linear correlation function $L(r)$ profiles derived from the original SAXS patterns and the fitted patterns of the net lamellar peak. Prominent fluctuations especially at r values of *ca*. 2 to 5 nm and *ca*. 7 to 10 nm were seen for the linear correlation function profiles originated from the total SAXS patterns (see **Fig. 4**). These fluctuations actually reflected the interference arising from the non-lamellar third-phase starch, which were undesired for accurately calculating the parameters of the semicrystalline lamellae (a two-phase structure). In contrast, when the fitted data of the net lamellar peak were used, the linear correlation function showed perfect profiles (see **Fig. 4**), which were very similar to that for lamellar semicrystalline polymers (Goderis, Reynaers, Koch & Mathot, 1999). Therefore, the profile of linear correlation function could be greatly improved by using the net lamellar scattering as the source data.

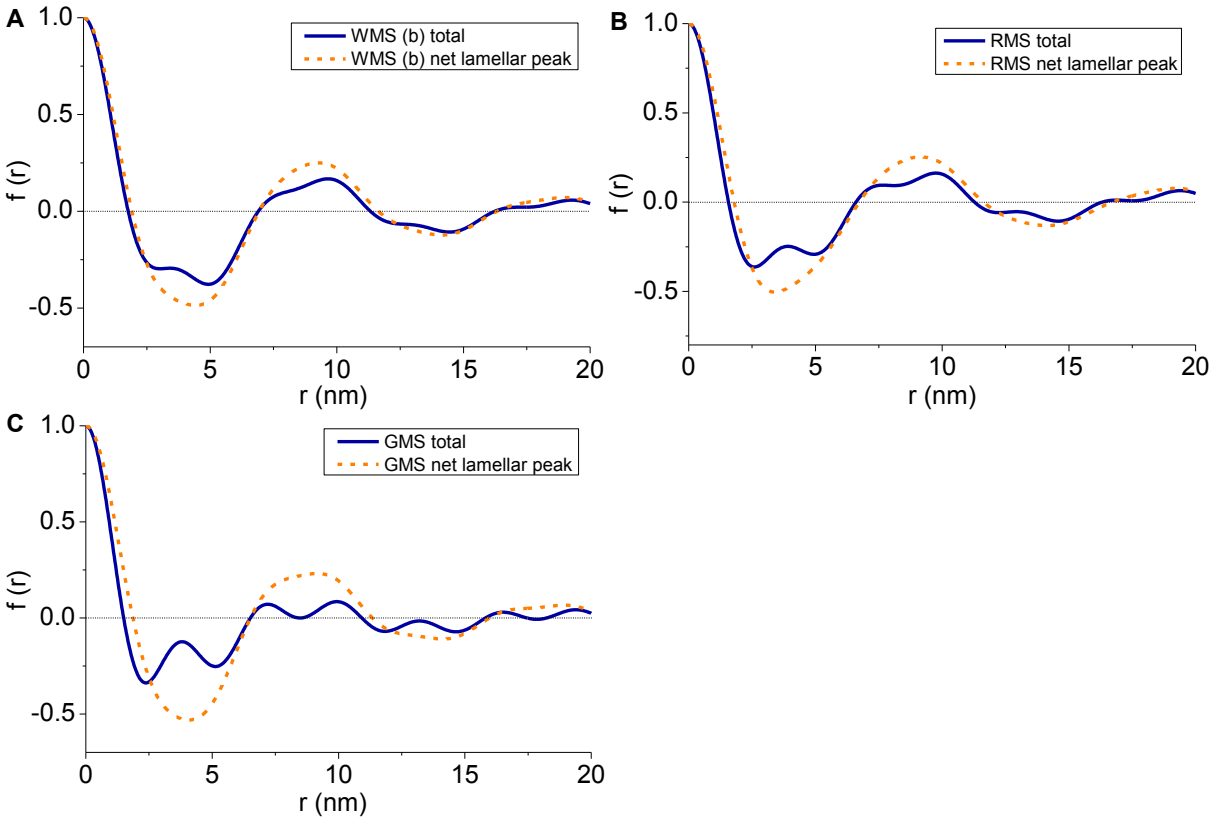

Fig. 4 Linear correlation function profiles derived from the total SAXS patterns and the net lamellar peak profiles for waxy maize starch with secondary fitting (WMS (b)), regular maize starch (RMS) and Gelose 50 high-amylose maize starch (GMS).

3.3 Quantitative analysis of starch lamellar parameters using the new method

The proposed method could not only resolve the net lamellar peak from the SAXS pattern but also remove the undesired fluctuations of the linear correlation function profile, which confirmed the applicability of this method for properly quantifying P_{SL} and other lamellar parameters for WMS, RMS and GMS. A test criterion was also provided for verifying the validity of the proposed fitting, *i.e.*, the almost tangency between *PL*+*B* profile and the whole SAXS pattern at a high *q* tail.

Table 1 shows the quantified lamellar parameters for WMS, RMS and GMS. The power-law exponent (α) in Eq. (4) was *ca.* 2, since the randomly-oriented system of starch lamellae has a q^{-2} dependence (Doutch & Gilbert, 2013; Zhang et al., 2015). P_{SL} values ranged from *ca*. 30% to 60%,

which had a same changing trend as that of X_c for WMS, RMS and GMS. The lamellar thicknesses, *i.e.*, d, d_c and d_a, were reasonable, but slightly different from previously reported values (Qiao et al., 2016; Zhang et al., 2015). This difference probably resulted from the removal of the scattering of non-lamellar amorphous starch, which was previously taken into account and interfered with the calculation of lamellar parameters using the linear correlation function.

Furthermore, the volume fraction (φ_c) of the crystalline components within the semicrystalline lamellae had a value of *ca*. 71–73%. The value of this parameter was slightly lower than that for a wheat starch acquired with the paracrystalline model (Cameron & Donald, 1993a). The ratio ($R_{X/\varphi}$) of X_c to φ_c was comparable to P_{SL}, which was consistent with the fact that the starch crystallites were predominantly packed in the semicrystalline lamellae. This similarity further confirmed the applicability of the new method to estimate P_{SL}.

3.4 Validity of the new method for analyzing starch semicrystalline lamellae with thickness distribution

As shown by above analyses, it was harder to resolve the lamellar scattering from the SAXS pattern for WMS than for RMS and GMS, using the proposed fitting with smallest reduced *chi*-square. Previous findings confirm that the thickness of starch semicrystalline lamellae distributes in a specific range that is positive to the width of the lamellar peak (Cardoso & Westfahl, 2010; Witt, Doutch, Gilbert & Gilbert, 2012; Zhang et al., 2015). As seen in **Fig. S2A** and S2**B** (supplementary data) and **Fig. 3C**, the sub-pattern of the net lamellar peak for RMS and GMS showed a single peak, whereas that for WMS exhibited an unresolved doublet. Namely, other than the lamellae indicated by a peak at *ca*. 0.65 $Å^{-1}$, there was a notable proportion of thicker lamellae in WMS, as shown by a shoulder at q values lower than 0.65 $Å^{-1}$. Here, it is reasonable to propose that the distribution of starch lamellae thickness substantially affected the fitting result for the three maize starches. The vast distribution of WMS lamellae thickness prevented the proposed fitting with smallest reduced *chi*-

square from accurately fitting the scattering of the lamellar structure. Therefore, while using the developed method to quantify the lamellar features of starch, the distribution of lamellar thickness must be considered. To address this, the developed method provides an assessment of the validity for the fitting based on Eq. (4), *i.e.*, the fitted *PL+B* profile should be almost tangent to its original SAXS pattern at a high *q* tail (around 0.2 $Å^{-1}$).

3.5 Validity of the new method for analyzing starches from different botanic origins

Fig. 5 shows the SAXS pattern, the resolved patterns and the linear correlation function profiles of PS. Following the proposed criterion, the *PL+B* profile of PS was nearly tangent to the total SAXS pattern at a high *q* tail (*cf.* **Fig. 5B**). Similar to that for WMS, the net lamellar peak profile of PS showed an unresolved doublet. The profile of linear correlation function for PS could be largely improved using the fitted scattering of the net lamellar peak. The related lamellar parameters of PS are recorded in **Table 1**. PS had a X_c comparative to previous findings (Lopez-Rubio, Flanagan, Gilbert & Gidley, 2008). The value of P_{SL} for PS was *ca*. 56% that was close to the ratio of X_c to φ_c, which was consistent with the cases for WMS, RMS, and GMS. The value of *d* for PS was slightly lower than that for maize starches, which agreed with previous studies (Witt, Doutch, Gilbert & Gilbert, 2012; Zhang, Zhao, Li, Li, Xie & Chen, 2014; Zhang et al., 2014). Also, other lamellar parameters of PS, such as d_a, d_c and φ_c, were reasonable. Hence, the proposed method in the present work was valid for evaluating the semicrystalline features of starches from different botanical origins.

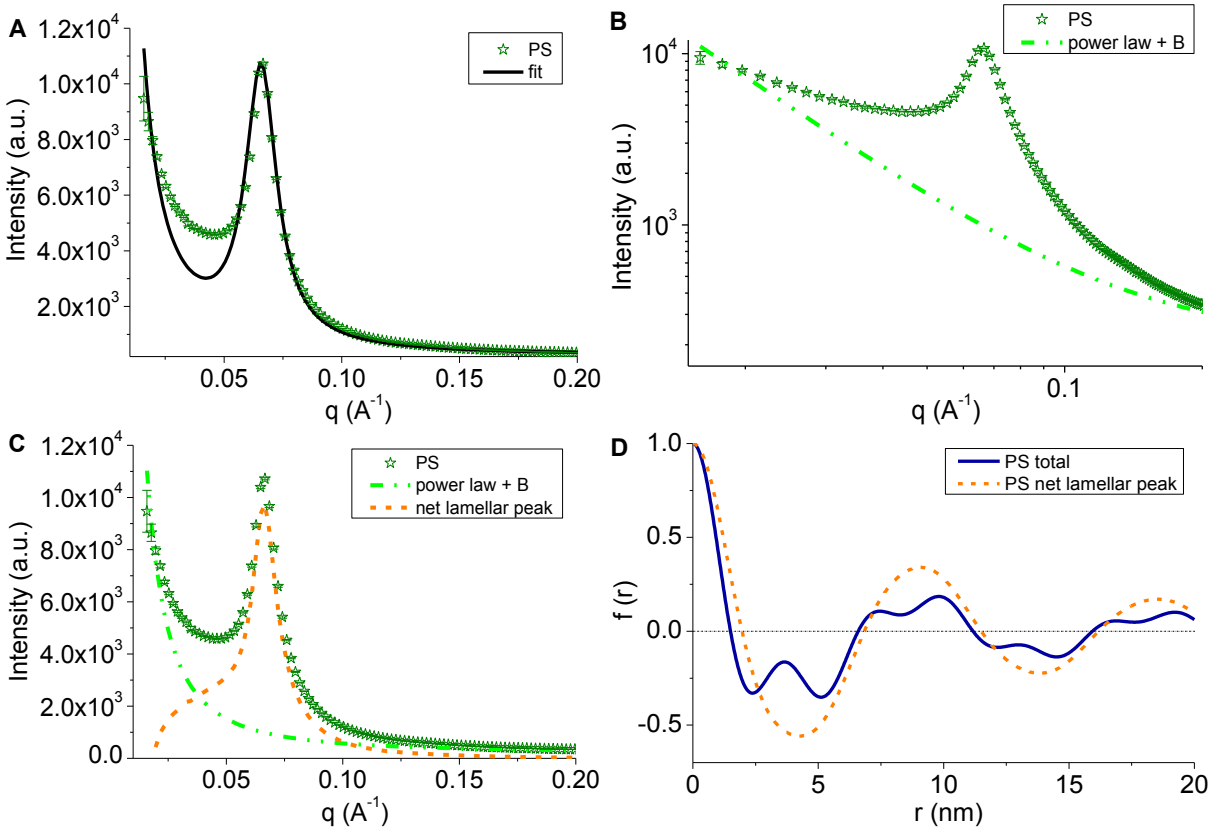

Fig. 5 SAXS pattern and its fit curve (A), SAXS pattern and its profile of power-law scattering *PL* plus scattering background *B* (B), decomposition of SAXS patterns into sub-patterns of net lamellar peak and *PL*+*B* (C), and linear correlation function profiles (D) for potato starch (PS).

In addition, it is worth mentioning that PS and GMS had a B-type crystalline structure, but WMS and RMS showed an A-type crystalline structure. While the B-type crystallites of starch contain 36 inter-helical water molecules in each hexagonal crystal unit with an open packing of helices, the A-type crystallites have only 8 water molecules in each monoclinic crystal unit with tightly packed helices (Zhang, Xiong, Li, Li, Xie & Chen, 2014). Thus, compared with WMS and RMS, PS and GMS had a different organization of starch helices in the crystal cells within the crystalline lamellae; though both A- and B-polymorphic starches have similar packing densities of crystalline (*ca*. 1.2 g/cm^3) and amorphous (*ca*. 0.5 g/cm^3) lamellae (Donald, Kato, Perry & Waigh, 2001; Perry & Donald, 2000). Nonetheless, with the proposed criterion, the fitting method here based on Eq. (4)

could properly resolve the scattering of lamellae and that of non-lamellar amorphous starch from the whole SAXS pattern for starches with different crystalline types.

4 Conclusions

This work proposes a fitting method to analyze SAXS data of starch granules to better calculate the parameters of starch semicrystalline lamellae, including the proportion of semicrystalline lamellae within the starch granule (P_{SL}), the thicknesses of semicrystalline (d), crystalline (d_c) and amorphous (d_a) lamellae, and the volume fraction (φ_c) of crystalline lamellae within the semicrystalline lamellae. For this purpose, the SAXS pattern was separated into sub-patterns of the net lamellar peak and the profile of power-law plus scattering background ($PL+B$) using a power-law function with two Gaussian plus Lorentz functions. The fitted scattering of the net lamellar peak was used to largely improve the profile of the linear correlation function. Accordingly, P_{SL}, φ_c and the lamellar thicknesses (d, d_c and d_a) were accurately calculated. It is worth noting that compared to the botanical origin, the distribution of lamellar thickness showed a more apparent effect on the validity of the proposed method. To ensure the validity of the developed method for resolving the lamellar scattering from the original SAXS pattern, a test criterion was proposed, *i.e.*, the total scattering pattern should be mostly tangent to its $PL+B$ profile at high q values. Hence, these results provide a basis for accurately linking the semicrystalline structure of starch to its functionalities.

Acknowledgements

The authors would like to acknowledge the Fundamental Research Funds for the Central Universities (2662016QD008), the Hubei Provincial Natural Science Foundation of China (2016CFB142), the Open Project Program of Provincial Key Laboratory of Green Processing Technology and Product Safety of Natural Products (No. 201604 and 201602), the National Natural Science Foundation of China (No. 31401586 and 31501520), and the Hunan Province Science and

Technology Key Project (2014FJ1008). This research was partly undertaken on the SAXS/WAXS beamline at the Australian Synchrotron, Victoria, Australia.

Reference

Blazek, J., & Gilbert, E. P. (2010). Effect of Enzymatic Hydrolysis on Native Starch Granule Structure. *Biomacromolecules, 11*(12), 3275-3289.

Buleon, A., Colonna, P., Planchot, V., & Ball, S. (1998). Starch granules: structure and biosynthesis. *International Journal of Biological Macromolecules, 23*(2), 85-112.

Cai, L., & Shi, Y. C. (2013). Self-assembly of short linear chains to A- and B-type starch spherulites and their enzymatic digestibility. *Journal of Agricultural and Food Chemistry, 61*(45), 10787-10797.

Cameron, R. E., & Donald, A. M. (1993a). A Small-Angle X-Ray-Scattering Study of Starch Gelatinization in Excess and Limiting Water. *Journal of Polymer Science Part B-Polymer Physics, 31*(9), 1197-1203.

Cameron, R. E., & Donald, A. M. (1993b). A Small-Angle X-Ray-Scattering Study of the Absorption of Water into the Starch Granule. *Carbohydrate Research, 244*(2), 225-236.

Cardoso, M. B., & Westfahl, H. (2010). On the lamellar width distributions of starch. *Carbohydrate Polymers, 81*(1), 21-28.

Daniels, D. R., & Donald, A. M. (2004). Soft Material Characterization of the Lamellar Properties of Starch: Smectic Side-Chain Liquid-Crystalline Polymeric Approach. *Macromolecules, 37*(4), 1312-1318.

Donald, A. M., Kato, K. L., Perry, P. A., & Waigh, T. A. (2001). Scattering studies of the internal structure of starch granules. *Starch-Stärke, 53*(10), 504-512.

Doutch, J., & Gilbert, E. P. (2013). Characterisation of large scale structures in starch granules via small-angle neutron and X-ray scattering. *Carbohydrate Polymers, 91*(1), 444-451.

Fuentes-Zaragoza, E., Sánchez-Zapata, E., Sendra, E., Sayas, E., Navarro, C., Fernández-López, J., & Pérez-Alvarez, J. A. (2011). Resistant starch as prebiotic: A review. *Starch-Starke, 63*(7), 406-415.

Goderis, B., Reynaers, H., Koch, M., & Mathot, V. (1999). Use of SAXS and linear correlation functions for the determination of the crystallinity and morphology of semi‐crystalline polymers. Application to linear polyethylene. *Journal of Polymer Science Part B: Polymer Physics, 37*(14), 1715-1738.

Jiang, Q. Q., Gao, W. Y., Li, X., & Zhang, J. Z. (2011). Characteristics of native and enzymatically hydrolyzed Zea mays L., Fritillaria ussuriensis Maxim. and Dioscorea opposita Thunb. starches. *Food Hydrocolloids, 25*(3), 521-528.

Juansang, J., Puttanlek, C., Rungsardthong, V., Puncha-arnon, S., & Uttapap, D. (2012). Effect of gelatinisation on slowly digestible starch and resistant starch of heat-moisture treated and chemically modified canna starches. *Food Chemistry, 131*(2), 500-507.

Liu, H., Xie, F., Yu, L., Chen, L., & Li, L. (2009). Thermal processing of starch-based polymers. *Progress in Polymer Science, 34*(12), 1348-1368.

Liu, W. C., Halley, P. J., & Gilbert, R. G. (2010). Mechanism of Degradation of Starch, a Highly Branched Polymer, during Extrusion. *Macromolecules, 43*(6), 2855-2864.

Lopez-Rubio, A., Flanagan, B. M., Gilbert, E. P., & Gidley, M. J. (2008). A novel approach for calculating starch crystallinity and its correlation with double helix content: a combined XRD and NMR study. *Biopolymers, 89*(9), 761-768.

Lopez-Rubio, A., Flanagan, B. M., Shrestha, A. K., Gidley, M. J., & Gilbert, E. P. (2008). Molecular rearrangement of starch during in vitro digestion: toward a better understanding of enzyme resistant starch formation in processed starches. *Biomacromolecules, 9*(7), 1951-1958.

Luengwilai, K., & Beckles, D. M. (2009). Structural investigations and morphology of tomato fruit starch. *Journal of Agricultural and Food Chemistry, 57*(1), 282-291.

Perez, S., & Bertoft, E. (2010). The molecular structures of starch components and their contribution to the architecture of starch granules: A comprehensive review. *Starch-Starke, 62*(8), 389-420.

Perry, P. A., & Donald, A. M. (2000). SANS study of the distribution of water within starch granules. *International Journal of Biological Macromolecules, 28*(1), 31-39.

Pikus, S. (2005). Small-angle x-ray scattering (SAXS) studies of the structure of starch and starch products. *Fibres & Textiles in Eastern Europe, 13*(5), 82-86.

Pu, H., Chen, L., Li, X., Xie, F., Yu, L., & Li, L. (2011). An oral colon-targeting controlled release system based on resistant starch acetate: synthetization, characterization, and preparation of film-coating pellets. *Journal of Agricultural and Food Chemistry, 59*(10), 5738-5745.

Qiao, D., Yu, L., Liu, H., Zou, W., Xie, F., Simon, G., Petinakis, E., Shen, Z., & Chen, L. (2016). Insights into the hierarchical structure and digestion rate of alkali-modulated starches with different amylose contents. *Carbohydrate Polymers, 144*, 271-281.

Situ, W., Li, X., Liu, J., & Chen, L. (2015). Preparation and Characterization of Glycoprotein-Resistant Starch Complex As a Coating Material for Oral Bioadhesive Microparticles for Colon-Targeted Polypeptide Delivery. *Journal of Agricultural and Food Chemistry, 63*(16), 4138-4147.

Tan, I., Flanagan, B. M., Halley, P. J., Whittaker, A. K., & Gidley, M. J. (2007). A method for estimating the nature and relative proportions of amorphous, single, and double-helical components in starch granules by C-13 CP/MAS NMR. *Biomacromolecules, 8*(3), 885-891.

Witt, T., Doutch, J., Gilbert, E. P., & Gilbert, R. G. (2012). Relations between molecular, crystalline, and lamellar structures of amylopectin. *Biomacromolecules, 13*(12), 4273-4282.

Xie, F., Halley, P. J., & Avérous, L. (2012). Rheology to understand and optimize processibility, structures and properties of starch polymeric materials. *Progress in Polymer Science, 37*(4), 595-623.

Zhang, B., Chen, L., Li, X., Li, L., & Zhang, H. (2015). Understanding the multi-scale structure and functional properties of starch modulated by glow-plasma: A structure-functionality relationship. *Food Hydrocolloids, 50*, 228-236.

Zhang, B. J., Chen, L., Xie, F. W., Li, X. X., Truss, R. W., Halley, P. J., Shamshina, J. L., Rogers, R. D., & McNally, T. (2015). Understanding the structural disorganization of starch in water-ionic liquid solutions. *Physical Chemistry Chemical Physics, 17*, 13860-13871.

Zhang, B. J., Xiong, S. X., Li, X. X., Li, L., Xie, F. W., & Chen, L. (2014). Effect of oxygen glow plasma on supramolecular and molecular structures of starch and related mechanism. *Food Hydrocolloids, 37*, 69-76.

Zhang, B. J., Zhao, Y., Li, X. X., Li, L., Xie, F. W., & Chen, L. (2014). Supramolecular structural changes of waxy and high-amylose cornstarches heated in abundant water. *Food Hydrocolloids, 35*, 700-709.

Zhang, B. J., Zhao, Y., Li, X. X., Zhang, P. F., Li, L., Xie, F. W., & Chen, L. (2014). Effects of amylose and phosphate monoester on aggregation structures of heat-moisture treated potato starches. *Carbohydrate Polymers*, *103*, 228-233.